



# **Accepted Article**

**Title:** Observation of the low frequency spectrum of water trimer as a sensitive test of the water trimer potential and the dipole moment surface

Authors: Martina Havenith-Newen, Raffael Schwan, Chen Qu, Devendra Mani, Nitish Pal, Gerhard Schwaab, Joel M. Bowman, and Gregory Tschumper

This manuscript has been accepted after peer review and appears as an Accepted Article online prior to editing, proofing, and formal publication of the final Version of Record (VoR). This work is currently citable by using the Digital Object Identifier (DOI) given below. The VoR will be published online in Early View as soon as possible and may be different to this Accepted Article as a result of editing. Readers should obtain the VoR from the journal website shown below when it is published to ensure accuracy of information. The authors are responsible for the content of this Accepted Article.

To be cited as: Angew. Chem. Int. Ed. 10.1002/anie.202003851

Link to VoR: https://doi.org/10.1002/anie.202003851

# Observation of the low frequency spectrum of water trimer as a sensitive test of the water trimer potential and the dipole moment surface

Raffael Schwan,<sup>[a]</sup> Chen Qu,<sup>[b]</sup> Devendra Mani,<sup>[a]</sup> Nitish Pal,<sup>[a]</sup> Gerhard Schwaab,<sup>[a]</sup> Joel M. Bowman,<sup>[b]</sup> Gregory Tschumper,<sup>[c]</sup> and Martina Havenith\*<sup>[a]</sup>

 Dr. R. Schwan, Dr. D. Mani, N. Pal, Dr. G. Schwaab, Prof. M. Havenith Physical Chemistry II, Department of Chemistry and Biochemistry Ruhr-Universität Bochum Bochum(Germany)

E-mail: martina.havenith@rub.de

[b] Dr. C. Qu, Department of Chemistry Biochemistry, University of Maryland, College Park, Maryland 20742, USA

[c] Prof. J. M. Bowman

Cherry L. Emerson Center for Scientific Computations and Department of Chemistry, Emory University Atlanta, Georgia 30322 (USA)

E-mail: jmbowma@emory.edu

[d] Prof. G. Tschumper

Department of Chemistry and Biochemistry University of Mississippi

Mississippi 38677 (USA)

Supporting information for this article is given via a link at the end of the document

Abstract: The intermolecular interaction of bulk water is dominated by pairwise and non-pairwise cooperative interactions, with the later accounting for ca. 25 % of the total energy.[1] Whereas by now accurate descriptions of the pairwise interaction are available, which can be tested by precise low frequency spectra of water dimer over the entire range up to 550 cm<sup>-1</sup>, the same does not hold for the threebody interactions. Here, we report the first comprehensive spectrum of the water trimer in the frequency region from 70 to 620 cm<sup>-1</sup>, using our helium nanodroplet isolation setup at the free-electron lasers FELIX in Nijmegen. By comparison to accompanying high level quantum calcualtions, we are able to assign the experimentally observed intermolecular bands. The transition frequencies of the degenerate translation, the degenerate in-plane, the non-degenerate out-of-plane libration as well as additional bands of the out-of-plane librational mode are reported for the first time. These provide a benchmark for state-of-the art water potentials and dipole moment surfaces, especially in respect to the three-body interaction. Furthermore, we are able to deduce the size of the torsional splitting in the excited intermolecular modes, which increase upon vibrational excitation.

#### Introduction

Water is the most prominent solvent and, therefore, of fundamental importance for chemistry and biology. However, despite decades of research, an accurate description of the underlying intermolecular interactions on a molecular level is still a scientific challenge. Spectroscopic studies, providing high-resolution spectra of intermolecular modes, in combination with ab initio calculations give access to the potential energy surface (PES) of water clusters. An essential objective of this research is the development of a universal water model from first principles, which is capable to predict the properties of water in all its forms and over a wide range of conditions.<sup>[6-10]</sup>

The binding energy of water in the solid and liquid phase has been found to be dominated by two-body interactions. [11-13] Whereas, water dimer is the ideal candidate to test the accuracy of water potential for an accurate description of two-body interaction, water trimer is the obvious candidate to test the three-body interactions, which are essential to describe accurately bulk water and ice. Initial studies focused on the accurate determination of an accurate water dimer potential energy surface. [14-25] The cyclic equilibrium structure of the water trimer is significantly stabilized by three-body interaction, which will aid in incorporating cooperativity into the description of water models.

The many body representation of the water potential has a long history, beginning with the seminal work of Stillinger and coworkers.  $^{[26]}$  This representation for N water monomers can be written as

$$\sum_{i=1}^{N} V_i + \sum_{i>i}^{N} \sum_{i=1}^{N} V_{ij} + \sum_{k>i}^{N} \sum_{j>i}^{N} \sum_{i=1}^{N} V_{ijk} + \dots$$

where  $V_i$  is the 1-body (monomer) potential of the ith monomer,  $V_{ij}$  is the 2-body interaction between monomers i and j,  $V_{ijk}$  the 3-body interaction between monomers i, j, k, etc. This representation is useful provided it converges quickly and ideally monotonically. This can be checked numerically by calculating the total electronic energy of N monomers, where by necessity N must be "small" where, "small" is determined by the level of ab initio theory used to obtain the electronic energy. For a high-level method such as CCSD(T) N is around 20. If we define the interaction action as the total electronic energy minus the energy of the 1-body monomers, these methods have shown that 2-body terms account for roughly 90% of the interaction energy. The 3-body terms account for roughly 8% of the remaining interaction energy. Thus, overall the 1-, 2- and 3-body energies account for roughly 98% of the total energy. [13, 27-29] Higher body

interactions, although small matter for energy ordering of isomeric forms of moderate-sized water clusters. The small 4 and higher-body interactions do appear to be well represented by classical polarization effects.

Fully ab initio approaches to obtain the 2-body interaction for rigid monomers began with the CC-pol potential, which is a fit to thousands of CCSD(T) electronic energies.[7] For flexible monomers the TTMn-F class of potentials was a major step in this direction. This potential used a sum of atom-atom exp-12 potential to represent the full 2-body (monomer) interaction with parameters fits to several hundred MP2 calculations. A fully ab initio "non-parametric" approach was taken by Huang et al.,[30] who fit tens of thousands of CCSD(T)/aug-cc-pVTZ electronic energies for the water dimer, using a fit basis of permutationally invariant polynomials (PIPs). This was already a significant challenge as this potential is 12 dimensional (actually 15 variables were used in the PIP fit.) The latest version of this dimer potential [22] was used in a recent publication from the authors focused on the IR spectrum of the water dimer in the far IR region.[31] The 2-body interaction mentioned above is obtained from this dimer potential. Shortly after the work by Huang et al., a PIP fit was done for the water trimer based on roughly 40 000 MP2/ aug-cc-pVTZ energies.[32] The 3-body interaction potential is obtained from this fit. In order to form an overall water potential, this 3-body contribution was combined with three other components: the two-body interaction from the dimer potential, the spectroscopically accurate H<sub>2</sub>O monomer potential of Partridge and Schwenke for the 1-body contributions, and the long-range portion of the TTM3-F potential for 4- and higherbody interactions. The result is referred to as the WHBB water potential.[33] Accurate dissociation energies of the water dimer and trimer were reported using WHBB and rigorous diffusion Monte Carlo calculations of the zero-point energies. These energies were validated by experiment. [34-35] Of special significance to this paper, was the determination that the intrinsic 3-body interaction accounts for roughly 25% of the dissociation energy,  $D_0$ .

An extensive review of *ab initio* water potentials, with a focus on the MB-Pol potential, has recently appeared and the interested reader is referred there. [36] Clearly, it is important to test the quality of these *ab initio* potentials. We do that here, using new experiments on the far IR spectrum of water trimer, which provide a comprehensive overview of the intermolecular fingerprint range between 80 and 600 cm<sup>-1</sup>. This is an extension of our recent work on the water dimer towards higher clusters. [31] The theoretical work consists of *ab initio* VPT2 calculations of fundamental energies. In addition, harmonic, scaled harmonic frequencies and fixed-node diffusion Monte Carlo (DMC) calculations of the splitting for the ground state are reported using the WHBB potential. Details of these calculations are given in the Supporting Information (SI). Harmonic frequencies using the MB-Pol potential are also given in the SI.

Water trimer has a cyclic equilibrium structure, with each water molecule serving as proton donor to one neighboring water molecule and as proton acceptor to the other. [37-44] In the equilibrium structure, two free hydrogen atoms are pointing upwards with respect to the O-O-O plane while the third is pointing downwards.. [45]

The water trimer vibrational spectrum consists of twelve intermolecular and nine intramolecular modes. The intermolecular modes are depicted in the SI. The spectrum is enriched by two low barrier tunneling motions (see Figure 1a). [46-49] The Molecular Symmetry group of the cyclic equilibrium

structure of water trimer is  $C_1(M)$ .<sup>[50]</sup> Proton interchange (without breaking any covalent bonds), results in 48 isoenergetic structures, which are connected via these two low-barrier tunneling pathways.

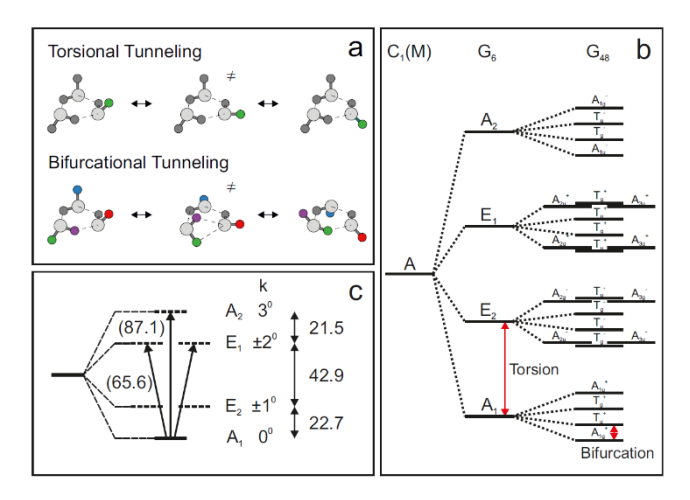


**Figure 1.** a) The two low-barrier tunneling pathways of water trimer. The torsional tunneling pathway changes the orientation of the free hydrogen atoms and the bifurcation tunneling pathway results in the exchange of the free and bound hydrogen atoms. b) Effect of the two low-barrier tunneling pathways on the energy levels of the water trimer. Due to the torsional tunneling pathway, each energy level is split into four energy levels labeled by the irreducible representations of the  $G_6$  MS group. Due to the bifurcational tunneling pathway, each energy level in the  $G_6$  MS group is further split into four energy levels labeled by the irreducible representations of the  $G_6$  MS group. On the Garrier split into four energy levels labeled by the irreducible representations of the  $G_6$  MS group. So that  $G_6$  MS group. So that  $G_6$  MS group is further split into four energy levels labeled by the irreducible representations of the  $G_6$  MS group. So that  $G_6$  MS group is further split into four energy levels abeled by the irreducible representations of the  $G_6$  MS group. So that  $G_6$  MS group is further split into four energy level in the  $G_6$  MS group is further split into four energy level in the  $G_6$  MS group is further split into four energy level in the  $G_6$  MS group is further split into four energy level in the  $G_6$  MS group. So the bifurcational tunneling pathway.

The first low-barrier tunneling pathway is denoted as flipping or torsional tunneling. Henceforth, we will refer to this tunneling pathway as torsional tunneling. Torsional tunneling changes the orientation of the free hydrogen atoms in the cyclic equilibrium structure of water trimer (see Figure 1a). If torsional tunneling is feasible, the corresponding MS group is  $G_6$ , which is isomorphic to the  $C_{3h}$  point group. Tunneling will cause a splitting of each energy level into four (two non-degenerate and two degenerate) vibrational-tunneling levels labeled according to the irreducible representations in the G<sub>6</sub> MS group (see Figure 1b). A qualitative energy diagram is displayed in Figure 1c. The states are labeled by torsional quantum numbers  $k = 0^{\circ}$ ,  $\pm 1^{\circ}$ ,  $\pm 2^{\circ}$  and  $3^{\circ}$ . The irreducible representations are  $A_1$ ,  $E_2$ ,  $E_1$ , and  $A_2$ , respectively. The following transitions are allowed from the ground state: A2  $\leftarrow A_1$  for parallel ( $\Delta K$ =0) transitions and  $E_1 \leftarrow A_1$  for perpendicular ( $\Delta K$ =1) transitions., implying that their total angular quantum number changes by  $\Delta |k-K| = 3$ .[3] In the ground state the torsional tunneling splittings are  $\beta_t$ :  $2\beta_t$ :  $\beta_t$ , which is characteristic for a cyclic potential with six isoenergetic minima. [46] In the ground state  $\beta_t$  was determined as 21-22 cm<sup>-1</sup>.[2-3, 51]

The second tunneling mode, the bifurcational tunneling describes an exchange of the free and bound hydrogen atoms (see Figure 1a). The bifurcation tunneling pathway results in a splitting of each energy level in the  $G_6$  MS group into four levels, which are labeled by irreducible representations in the  $G_{48}$  MS group (see Figure 1b). The bifurcational tunneling splitting In the ground state this tunneling splitting is very small, i.e. in the order of few MHz. [52]

The calculation of excited state tunneling splittings is a major challenge for theory. These must reply on a potential energy surface that accurately describes the large amplitude motion connecting equivalent minima, and the saddle point, udp, separating them. Fortunately the WHBB PES does describe this accurately, i.e., the saddle point energy is  $83.2\ cm^{-1}$  in very good agreement with the benchmark value of  $81.5\ cm^{-1}.^{[53]}$  To further test the accuracy of the WHBB PES for tunneling splittings, we performed fixed node diffusion Monte Carlo (DMC) calculations of the splitting for the ground state (details are given in Supporting Information (SI)). The result of  $26\pm 5\ cm^{-1}$  is in good agreement with the experimental value of ca. 22 cm $^{-1}.^{[1]}$  Unfortunately, the calculation of tunneling splittings for excited states using the DMC approach is not straightforward, but could be the focus of future research.

Pioneering high resolution gas phase studies have been carried out by the Saykally group. Due to a lack of laser sources in the so-called THz gap these studies predominantly focused on the frequency region below 100 cm<sup>-1</sup>.<sup>[2-3, 51, 54-59]</sup> This region is dominated by a manifold of torsional states of the water trimer.<sup>[60]</sup> For the torsional modes, a harmonic approximation has been found to be inappropriate and a pseudo-rotational model has been proposed.<sup>[45]</sup> These two low-barrier tunneling pathways are expected to couple strongly with the intermolecular modes of the water trimer, causing an anomalous tunneling pattern in the excited states. High resolutions studies of intermolecular modes have been restricted to few examples including the observation of the translational band of the (D<sub>2</sub>O)<sub>3</sub> isotopologue at 142.8 cm<sup>-1</sup> and the out-of-plane librational band of the (H<sub>2</sub>O)<sub>3</sub> isotopologue at approximately 520 cm<sup>-1</sup>.<sup>[4-5, 61]</sup>

Helium nanodroplet isolation spectroscopy is a versatile approach to infrared spectroscopic investigations of molecules and molecular aggregates.  $^{[62-66]}$  The technique enables stepwise aggregation and the spectroscopic characterization of molecular aggregates with well-defined cluster sizes at ultracold temperatures of 0.37 K. $^{[67]}$  Initially, the helium nanodroplet isolation technique was used to study water monomer as well as small water clusters ( $H_2O$ )<sub>n</sub> with n=2,3,4,5,6 in the region of the intramolecular O-H stretching mode. $^{[68-71]}$  and in the region of the intramolecular H-O-H bending mode $^{[72]}$ . Most recently, we presented benchmark measurements of the low frequency spectrum of the water dimer in Helium nanodroplets in the frequency range from 50 to 500 cm $^{-1}$ . $^{[31]}$ 

## **Experimental results and discussion**

Here, we report the first comprehensive low frequency study of the water trimer including the translational mode ( $R_i$ ), the inplane librational modes ( $\Phi_i$ ) and the out-of-plane librational modes ( $\beta_i$ ). The measurements were carried out at the BoHENDI helium nanodroplet isolation set-up at the free-electron lasers at the FELIX laboratory in Nijmegen. [73]

In Helium Nanodroplet Ionization (Hendi) spectroscopy the absorption is measured indirectly as the depletion of the ion current of a certain ionic fragment in the mass spectrum upon excitation of the embedded solute. In the present study, we investigate water trimer which are formed after sequential pickup of single water molecules. The depletion spectrum of small water clusters with an average pickup of 2–3 water molecules was recorded in the frequency region from 70 to 620 cm<sup>-1</sup>; see [31] for details. Depletion was detected at m/z = 19, which was

found to be highly selective for water dimer as well as water trimer. Bands which were assigned to water trimer were found in the following frequency range: 151-282 cm $^{-1}$ , 313-317 cm $^{-1}$ , 352-435 cm $^{-1}$  and 515-577 cm $^{-1}$ .

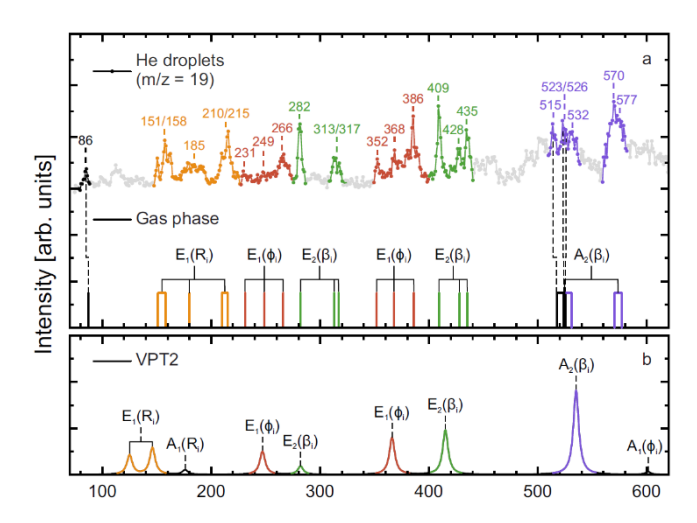


**Figure 2.** Comparison of our experimental FIR/THz water trimer  $(H_2O)_3$  spectrum (a, upper trace) with results from gas phase studies<sup>[2-5]</sup> (a, lower trace) and results from VPT2 calculations (b). The band origins determined from gas phase studies are represented as black sticks while those determined in the present study are shown as yellow, red, green and violet sticks. Dashed lines indicate bands also observed in gas phase studies. In the lower trace we plot results from VPT2 calculations, each mode was assigned following the notation of the  $G_6$  MS group as discussed in the text.

In Figure 2 we display an overview of the recorded low frequency spectrum of water cluster in helium nanodroplets in grey. Bands assigned to the translational mode ( $R_i$ ), in-plane librational modes ( $\Phi_i$ ) and out-of-plane librational modes ( $\beta_i$ ) are highlighted. A definitive assignment of the cluster size is based on pressure dependent intensity measurements, so-called pick-up curves. These were recorded at 86, 151, 158, 162, 185 210, 215, 266, 282, 313, 317, 352, 368, 386, 409, 428, 435, 515, 532, 570, and 577 cm<sup>-1</sup>, and I n case of the overlapping signals at 523 and 526 cm<sup>-1</sup>, one a pickup curve at 524 cm<sup>-1</sup>, see SI for details.

The pressure dependence of the signal at  $86 \text{ cm}^{-1}$ , follows a Poisson distribution with contributions from water dimer as well as water trimer. [31] The same ambiguity holds for the band at  $185 \text{ cm}^{-1}$ , which clearly shows contributions from several  $(H_2O)_n$  cluster, with partial contributions of n=3. Unfortunately, due to the low intensity of signals at 231 and 249 cm<sup>-1</sup> we were unable to obtain conclusive pickup curves.

All transitions as observed before in high resolution gas phase studies of the Saykally group are shown as dashed line .<sup>[2-5]</sup> In Figure 2b, lower trace, we display the predicted band center of our *ab initio* calculations based on vibrational perturbation theory of second order (VPT2).

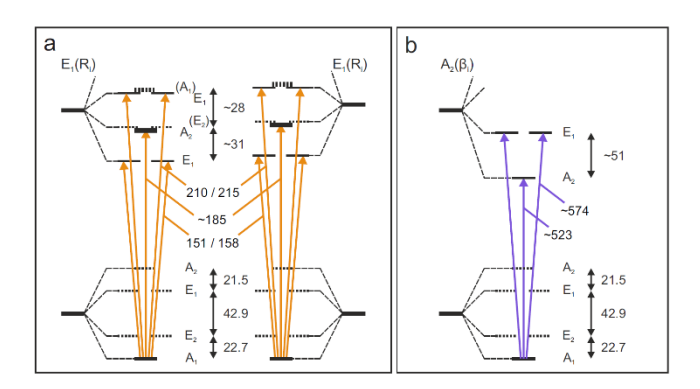


**Figure 3.** Qualitative energy level diagrams for the degenerate translations  $E_1(R_i)$  (a) and the non-degenerate out-of-plane libration  $A_2(\beta_i)$  (b). Observed transitions are indicated by solid arrows along with the observed experimental frequencies. All values are given in cm<sup>-1</sup>.

In the following, each intermolecular mode is assigned to a specific symmetry in  $G_6$  ( $A_1$ ,  $A_2$ ,  $E_1$  or  $E_2$ ). Due to torsional tunneling, each intermolecular mode will split into four distinct states (see Figure 1 for the ground state). Our experimental frequency resolution is on the order of ~0.5-2 cm<sup>-1</sup>, which is well below the torsional tunneling splitting, but exceeds by far the bifurcational tunneling splitting (few MHz in the ground state). This implies that while we are able to resolve the torsional tunneling splitting, the bifurcational splitting cannot be resolved, unless it is increased by several orders of magnitude upon vibrational excitation.

The water trimer is a symmetric-top molecule with gas phase rotational constants of A = B = 0.22 and C = 0.12 cm<sup>-1</sup>.[ $^{2-3}$ ,  $^{51}$ ] Due to the helium environment, the rotational constants are expected to be reduced by a factor of three.[ $^{66}$ ] Thus, distinct rotational transitions states cannot be resolved. At the temperature of 0.37 K, only the lowest torsional state (*i.e.*  $k = 0^{0}$ ) is expected to be populated. Based on the transitions rules, only parallel transitions ( $\Delta K = 0$ ) from the lowest populated  $k = 0^{0}$  torsional state to states with overall vibrational torsional  $A_{2}$  symmetry or perpendicular transitions ( $\Delta K = 1$ ) to states with an overall vibrational torsional  $E_{1}$  symmetry are allowed.

In our previous paper we presented theoretical spectra for the water dimer. The most rigorous (and complex) theoretical spectrum came for fully-coupled quantum calculations using the WHBB potential and dipole moment surfaces. Standard double harmonic calculations of the spectrum were also given and so anharmonic/coupled mode effects could be estimated by comparison of these two spectra. A simple scaling by a factor of 0.8 of the harmonic stick spectrum could be made to bring the scaled spectrum into accord with the rigorous one. Assuming transferability to the trimer, we use that scale factor here for the WHBB harmonic frequencies. Fortunately, new direct *ab initio* VPT2 energies were also obtained for the trimer. These results

are summarized in Table 1 along with experimental results. The intensity is from the double harmonic calculations using the WHBB dipole moment surface. A comparison of the WHBB harmonic frequencies given in this table are compared with previous direct CCSDT:MP2/haQZ ones as well as MB-Pol ones (see SI), shows agreement to within 0-10 cm<sup>-1</sup>. In the following we will use these predictions for an assignment of the observed bands.

Below 100 cm<sup>-1</sup>, centered at 86 cm<sup>-1</sup>, we observe one band, which is assigned to the  $k=3^0\leftarrow0^0$  perpendicular band in the ground state, in excellent agreement with results from gas phase VRT studies, which yielded a band origin of 87.1 cm<sup>-1</sup>.<sup>[2-3]</sup> The frequency range between 80 and 100 cm<sup>-1</sup> is dominated by dimer lines at 86 cm<sup>-1</sup> and at 99 cm<sup>-1</sup>. So even so the torsional band  $\tau_1$  is predicted at 101 cm<sup>-1</sup> (see Tab. 1) we are unable to observe this band.

In the frequency range between 100 and 220 cm<sup>-1</sup>, we observe three new broad signals centered at 156, 185, and 213 cm<sup>-1</sup>. The absorption peaks at 151/158 cm<sup>-1</sup> and 210/215 cm<sup>-1</sup> have a similar intensity and substructure; each shows two overlapping peaks separated by 5/6 cm<sup>-1</sup>. Based on comparison to the accompanying VPT2 calculations we assign these to the two perpendicular vibrational-tunneling transitions to the degenerate asymmetric translations  $E_1(R_i)$ . Note that in the global minimum only perpendicular transitions are allowed. At the {uud} stationary point the transition dipole moment is expected to have also parallel component, nevertheless perpendicular transitions are predicted to be more intensive.

We attribute the splitting of 7 cm<sup>-1</sup> between the bands at 151/158 cm<sup>-1</sup> and the splitting of 5 cm<sup>-1</sup> between the two bands of 210/215 cm<sup>-1</sup> to a splitting of the previously degenerate  $E_1(R_1)$  modes upon vibrational excitation. Based on our VPT2 calculations these are should be separated by 15 cm<sup>-1</sup> (see Table 1). In a previous lower-level calculation by Klopper *et al.*, a splitting of 7 cm<sup>-1</sup> is predicted, in very good agreement with the experiment.<sup>[74]</sup>

The two perpendicular transitions of the  $E_1(R_i)$  mode at 151/158 cm<sup>-1</sup> and 210/215 cm<sup>-1</sup> are separated by  $3\beta_t$ . Thus, based upon our experimental results, we deduce a torsional tunneling splitting of  $\beta_t$  ~19/20 cm<sup>-1</sup> which agrees well with the torsional tunneling splitting in the ground state. Based on this result, weaker parallel transitions are predicted around 170 to 180 cm<sup>-1</sup>. These might contribute to the broad absorption centered around 185 cm<sup>-1</sup>. Unfortunately, other bands as well as other water cluster also contribute to this band, which makes an unambiguous assignment for the band at 185 cm<sup>-1</sup> impossible.

Also the  $A_1(R_i)$  band at 185 cm<sup>-1</sup>, which is predicted to have a small intensity might contribute to the small broad peak at 185 cm<sup>-1</sup>.

Table 1. Comparison of experimental results (cm<sup>-1</sup>) with results from indicated calculations (cm<sup>-1</sup>). Each mode at the {udu} global minimum is assigned to its symmetry in the  $G_6$  MS group

Mode	Theory				Experiment He Nanodroplet		Experiment Gas Phase
	Harmonic <sup>a</sup>	Scaled Harmonic <sup>b</sup>	VPT2°	Intensity	v	β	
K= 3°←0°					<b>86</b> (⊥)	22 .[1]	87.1 .[2-3]
<i>T</i> 1	166	128	101	22	-	-	_
$E_1(R_i)$	177	141	139	21	151(⊥)/210(⊥)	20	-
E1(Ri)	185	148	154	29	158(±)/215(±)	19	-
<b>T</b> 2	195	157	152	10	-		-
$A_1(R_i)$	215	172	175	8	185 (?)		-
<b>7</b> 3	234	184	185	5	-	-	-
$E_1(\Phi_i)$	332	268	266	25	266(⊥)		-
$E_2(\beta_i)$	345	276	282	9	282(⊥)/313,317 (⊥)		-
E1(Φi)	431	347	358	40	352/368/386		-
$E_2(\beta_i)$	551	448	416	48	409(1),428/435 (1)		-
$A_2(\beta_i)$	644	516	564	91	515, 523, 526, 532 (  ) 570,577(⊥)	49	517.2, 523.9, 525.3 [8]
$A_1(\boldsymbol{\Phi}_{\mathrm{i}})$	833	662	670	3	_	_	_

a,bWHBB Ref.[33], cPresent results

In the frequency region between 220 and 440 cm<sup>-1</sup> we observe peaks at 231, 249, 266, 282, 313, 317, 352, 368, 386, 409, 428, and 435 cm<sup>-1</sup>. By comparison to our VPT2 calculation we attribute these to transitions to the degenerate in-plane libration  $E_1(\Phi_i)$  predicted at 266 and 358 cm<sup>-1</sup> and to the degenerate out-of-plane libration  $E_2(\beta_i)$  predicted at 282 and 416 cm<sup>-1</sup> (Figure 4). Note, that in the present case  $E_1(\Phi_i)$  and  $E_2(\beta_i)$  will mix at the {uud} stationary point. For  $E_1(\Phi_i)$  and  $E_2(\beta_i)$  modes two perpendicular vibrational-torsional transitions and one parallel transitions is allowed, however, perpendicular transitions are predicted to have a higher intensity.

By comparison to our VPT2 calculations, we assign the peaks at 231/249/266 cm<sup>-1</sup> and 352/368/386 cm<sup>-1</sup> tentatively to transitions to the degenerate in plane libration  $E_1(\Phi_i)$ . Both sets show a similar intensity pattern and are found in close proximity to the predicted band center. Whereas the peaks at 231/249 cm<sup>-1</sup> are very small and do not allow an unambiguous cluster assignment, the signal at 266 cm<sup>-1</sup> can clearly be attributed to  $(H_2O)_3$ . This peak is assigned to the perpendicular transition to the  $E_1(\Phi_i)$  mode with an overall torsional vibrational symmetry of  $E_1 \otimes E_1 = 2A_1 \oplus E_1$ . The same holds for the intense peak at 386 cm<sup>-1</sup>. Note, that that both states might be split into further however, overlapping peaks.

The peaks at 352 and 368 cm<sup>-1</sup> are tentatively assigned to parallel and perpendicular transitions to the lower lying torsional states of the in plane libration  $E_1(\Phi_i)$  mode, predicted at 358 cm<sup>-1</sup>. Due to the strong mixing of  $E_1(\Phi_i)$  and  $E_2(\beta_i)$ , we cannot anticipate a regular torsional tunneling pattern. Therefore, we

abstain from deducing a  $\beta_t$  value. Instead, we show the deduced energy level diagram in Figure 4.

In the same way, we assign the signals at 282 cm<sup>-1</sup> and 313/317 cm<sup>-1</sup> as well as 409 and 428/435cm<sup>-1</sup>, to the four perpendicular transitions to the two degenerate out-of plane librations ( $E_2(\beta_i)$ )

We speculate that the experimentally observed smaller splitting of 4 and 7 cm<sup>-1</sup> can be attributed to an increased bifurcational tunneling splitting upon vibrational excitation, similar as was proposed before for the out of plane  $A_2(\beta_i)$  librational mode. <sup>[8]</sup>.

In the frequency range above 500 cm<sup>-1</sup> two intermolecular modes are predicted based on our VPT2 calculations: The out-of-plane liberation  $A_2(\beta_i)$ , is predicted at 564 cm<sup>-1</sup> and the in-plane librational mode  $A_1(\Phi_i)$  at 670 cm<sup>-1</sup>. Since the  $A_1(\Phi_i)$  mode is expected to have a 30x smaller intensity than the  $A_2(\beta_i)$  band (see Tab. 1), we assign all peaks above 500 cm<sup>-1</sup> to parallel and perpendicular transitions to the out-of-plane libration,  $A_2(\beta_i)$ .

The first three experimentally observed peaks at 515, 523/526, and 532 cm<sup>-1</sup> are in excellent agreement with the previously observed bands origins at 517.2, 523.9 and 525.3 cm<sup>-1</sup> in a high resolution gas phase study <sup>[8]</sup> These were tentatively assigned to parallel transition from the ground state to the  $A_2(\beta_i)$  out of plane librational mode with a resolved bifurcational tunneling splitting. The bifurcational splits each state in a quartet, out of which three have been observed (assigned to  $A_2$ ,  $T_1$  and  $T_2$  components). <sup>[75]</sup> They attributed the splitting between the band centers at 517.2, 523.9 and 525.3 cm<sup>-1</sup> to the bifurcational tunneling splitting, implying that the latter is increased by three orders of magnitude upon librational excitation. <sup>[8]</sup>

We assign the peak at 532 cm<sup>-1</sup> to the fourth bifurcational tunneling component of the parallel transition to the out-of-plane libration, (the  $A_1^+$  subband), which has not been detected before. For transitions from  $K^* = 0$ , this fourth component of the quartet is expected to be a factor of 3, 9 and 11x smaller than each of the other components. However, if we sum over all  $K^*$  states (since we lack rotational resolution), their intensities become comparable.

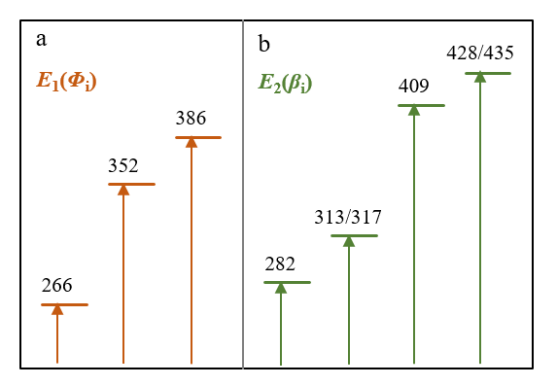


**Figure 4.** Qualitative energy level diagrams for the observed torsional states of the split degenerate in-plane librations  $E_1(\Phi_l)$  (a) and the degenerate out-of-plane librations  $E_2(\beta_l)$  (b). Due to strong mixing between  $E_1(\Phi_l)$  and  $E_2(\beta_l)$  an unambiguous assignment is not possible, as discussed in the text.

In our study we not only report the center frequency of the fourth tunneling component at 532 cm<sup>-1</sup> for the first time, but we can state that the pattern is no longer equally spaced – as in the ground state. In the ground state, the bifurcational tunneling can be explained by a single flip arrangement, with an excitation energy well below the tunneling barrier.<sup>[4-5]</sup> This approximation obviously does not hold any longer.

We also observe a second, broad band with a substructure centered at 570 and 570 cm<sup>-1</sup> (see Figure 2). These peaks are assigned to perpendicular transitions to the intermolecular  $A_2(\beta_i)$ mode, reported here for the first time. Previously, the bifurcational and the torsional splittings were postulated to be of the same order of magnitude (-3.1 and -2.3 cm<sup>-1</sup> or 1.6 and 4.6 cm<sup>-1</sup>). Based on our study we are now able to deduce the size of the torsional tunneling splitting in the vibrational excited  $A_2(\beta_i)$ mode. The difference between the center frequencies of parallel and perpendicular transition in this mode amount to  $\beta_t$  = 49 cm<sup>-</sup> <sup>1</sup>, which is one order of magnitude larger than the bifurcational tunneling splitting (ca. 8 cm<sup>-1</sup>).  $\beta_t$  is increased by a factor of more than two compared to the ground state and thus larger than previously anticipated. The magnitude of the bifurcational tunneling in the vibrational excited  $A_2(\beta_i)$  mode can be deduced from the difference between the first and fourth component of the quartet, i.e. the 517 cm<sup>-1</sup> and 532 cm<sup>-1</sup> peak:  $2\beta_b = (532-517)$ cm<sup>-1</sup>; thus  $\beta_b = 8.5$  cm<sup>-1</sup>. We confirm that the bifurcation tunneling splitting is increased by more than three orders of magnitude compared to the ground state, but  $\beta_t > \beta_b$  still holds. Both tunneling motions, albeit to different extent, are strongly coupled to the out-of-plane librational mode.

It is also interesting to note, that the bifurcational tunneling quartet is obviously more closely spaced in the perpendicular transition, observed between 570 and 577 cm<sup>-1</sup>, than in the case of parallel transitions, observed between 515 and 532 cm<sup>-1</sup>.

In contrast, in the ground state, the observed splitting is the same for the parallel as well as the perpendicular transition. If the splitting is dominantly caused by the coupled single flip bifuractional matrix elements, then we expect a splitting of  $\beta_b$  =  $8\beta_{1f1b}$  for parallel transition and  $\beta_b$  =  $4\beta_{1f1b}$  in case of perpendicular transitions. The experimentally observed difference for parallel transitions amounts to 17 cm $^{-1}$ . Hence, we deduce a value of  $\beta_{1f1b}$  = 2.125 cm $^{-1}$ . The anticipated maximum splitting for perpendicular transitions would then amount to  $4\beta_{1f1b}$  = 8.5 cm $^{-1}$ , which is in – within our experimental uncertainty – in very good agreement with the experimentally observed splitting of (577-570) cm $^{-1}$  = 7 cm $^{-1}$ .

To conclude this section, we note calculations of the ground-vibrational-state tunneling splitting in the water trimer using the ring-polymer instanton (RPI) method. [76-78] These used the WHBB potential [76-78] and MB-Pol potential. [77] The calculated splitting of about 50 cm $^{-1}$ , using either potential, is more than a factor of two larger than experiment. However, in recent work of Vaillant et al., [77] a splitting of (26  $\pm$  2) cm $^{-1}$  was obtained using a more rigorous PIMD approach, with the MB-Pol potential. This splitting is in very good agreement with the present DMC fixed-node splitting of (26  $\pm$  5) cm $^{-1}$  using WHBB, and both results are in good agreement with experiment. This indicates that these ab initio potentials can be used to obtain accurate tunneling splittings provided they are used with rigorous calculations of the splittings.

#### Conclusion

We report the first comprehensive FIR/THz spectrum of water trimer in the frequency region from 80 to 600 cm $^{-1}$ . Excellent agreement with previous high resolution gas phase studies, which were limited to the torsional mode  $r_1$  at 86 cm $^{-1}$  and the librational mode around 520 cm $^{-1}$  show that the influence of the helium nanodroplet environment can be neglected within our experimental resolution (ca. 1 cm $^{-1}$ ), similar as was observed before for the water dimer.<sup>[31]</sup>

Based on a comparison of the experimentally observed transitions with predictions from VPT2 predictions, we are able to assign the following intermolecular modes, with partially resolved torsional and even bifurcational tunneling splitting: The degenerate translation  $E_1(R_i)$ , the non-degenerate out-of-plane libration  $A_2(\beta_i)$ , two degenerate in-plane librations  $E_1(\Phi_i)$ , and two degenerate out-of-plane librations  $E_2(\beta_i)$ . These energies provide an excellent test for any state-of-the art water trimer potential.

We note that the torsional tunneling splitting is sensitive to the intermolecular excitation: For the degenerate translation  $E_1(R_i)$  mode the torsional tunneling splitting amounts to 20 cm<sup>-1</sup>, close to the value in the ground state. For the  $A_2(\beta_i)$  mode above 500 cm<sup>-1</sup>, the torsional tunneling splitting has increased to 49 cm<sup>-1</sup>. Due to the coupling of the  $E_1(\Phi_i)$  and  $E_2(\beta_i)$  mode, the torsional tunneling pattern is affected, thus we abstain from deducing a value for the torsional splitting  $\beta_t$ .

For the out-of-plane libration we observe all components of the bifurcation tunneling quartet, and confirm the previously proposed increase in tunneling splitting by several orders of magnitude. [4-5]

We tentatively assign the splitting in the degenerate out-of-plane libration  $E_2(\beta_i)$  mode of 4 cm<sup>-1</sup> (317-313 cm<sup>-1</sup>) and 7 cm<sup>-1</sup> at (435-428) cm<sup>-1</sup> to a bifurcational tunneling splitting. The

increase in bifurcational tunneling splitting will depend on the actual tunneling path, i.e. whether the intermolecular mode and the bifuractional tunneling mode are strongly coupled (are along the same coordinate) and on the energy of excitation in comparison to the tunneling barrier.

When computing the projections of the uud normal modes onto the bifurcational mode we find that both projections, for the  $E_2(\beta_i)$  as well as the  $E_1(R_1)$  are in the same order of magnitude as in case of the  $A_2$  ( $\beta_i$ ) mode (see SI). While we can speculate that experimentally, at 386 cm<sup>-1</sup> also a substructure can be resolved, it is more prominent in case of the out-of-plane librations. This might indicate, that the bifurcational tunneling pathway involves an out-of-plane mode. The observed increase in bifurcation tunneling towards higher frequencies can be attributed to the higher vibrational excitation energy, which results in an effective reduction of the tunneling barrier.

Up to now, torsional states of water trimer have been treated with a three-dimensional model, [60, 79] which reproduce the energies of the torsional states with k = 0, 1, 2, and 3. However, to describe the manifold of torsional states for the translational and librational modes accurately, a treatment of the water trimer in a twelve-dimensional model (*i.e.* including all twelve intermolecular modes) is inevitable. This remains one of the challenges of future theoretical studies.

## Acknowledgements

This work was funded by the Deutsche Forschungsgemeinschaft (DFG, German Research Foundation) under Germany's Excellence Strategy – EXC 2033 – 390677874 – RESOLV. The FELIX laboratory is funded by the Stichting voor Fundamenteel Onderzoek der Materie (FOM) and LASERLAB-EUROPE grant 654148. The theoretical work at Emory was supported by NASA, Grant No NNX16AF09G. The theoretical work at the University of Mississippi was carried out with support from the National Science Foundation under grant number CHE-1664998 and the computational resources provided by the Mississippi Center for Supercomputing Research.

Keywords: water cluster, water potentials, helium nanodroplet

- [1] F. N. Keutsch, J. D. Cruzan, R. J. Saykally, *Chemical reviews* 2003, 103, 2533-2578.
- [2] K. Liu, J. G. Loeser, M. J. Elrod, B. C. Host, J. Rzepiela, N. Pugliano, R. J. Saykally, *Journal of the American Chemical Society* 1994, 116, 3507-3512
- [3] E. Olthof, A. Van der Avoird, P. Wormer, K. Liu, R. Saykally, The Journal of chemical physics 1996, 105, 8051-8063.
- [4] F. N. Keutsch, R. S. Fellers, M. R. Viant, R. J. Saykally, *The Journal of Chemical Physics* 2001, 114, 4005-4015.
- [5] F. N. Keutsch, R. S. Fellers, M. G. Brown, M. R. Viant, P. B. Petersen, R. J. Saykally, *Journal of the American Chemical Society* 2001, 123, 5938-5941.
- [6] N. Goldman, C. Leforestier, R. Saykally, Philosophical Transactions of the Royal Society A: Mathematical, Physical and Engineering Sciences 2004, 363, 493-508.
- [7] R. Bukowski, K. Szalewicz, G. C. Groenenboom, A. Van der Avoird, Science 2007, 315, 1249-1252.
- [8] V. Babin, C. Leforestier, F. Paesani, Journal of chemical theory and computation 2013, 9, 5395-5403.

- [9] V. Babin, G. R. Medders, F. Paesani, Journal of chemical theory and computation 2014, 10, 1599-1607.
- [10] G. R. Medders, V. Babin, F. Paesani, Journal of chemical theory and computation 2014, 10, 2906-2910.
- [11] S. S. Xantheas, The Journal of chemical physics 1994, 100, 7523-7534
- [12] J. K. Gregory, D. C. Clary, The Journal of Physical Chemistry 1996, 100, 18014-18022.
- [13] M. P. Hodges, A. J. Stone, S. S. Xantheas, The Journal of Physical Chemistry A 1997, 101, 9163-9168.
- [14] C. Millot, A. J. Stone, Molecular Physics 1992, 77, 439-462.
- [15] R. S. Fellers, C. Leforestier, L. Braly, M. Brown, R. Saykally, *Science* 1999, 284, 945-948.
- [16] E. M. Mas, R. Bukowski, K. Szalewicz, G. C. Groenenboom, P. E. Wormer, A. van der Avoird, *The Journal of Chemical Physics* 2000, 113 6687-6701
- [17] G. Groenenboom, P. Wormer, A. Van Der Avoird, E. Mas, R. Bukowski, K. Szalewicz, The Journal of Chemical Physics 2000, 113, 6702-6715.
- [18] N. Goldman, R. Fellers, M. Brown, L. Braly, C. Keoshian, C. Leforestier, R. Saykally, The Journal of chemical physics 2002, 116, 10148-10163.
- [19] C. Leforestier, F. Gatti, R. S. Fellers, R. J. Saykally, The Journal of chemical physics 2002, 117, 8710-8722.
- [20] G. S. Tschumper, M. L. Leininger, B. C. Hoffman, E. F. Valeev, H. F. Schaefer III, M. Quack, *The Journal of chemical physics* 2002, 116, 690-701.
- [21] X. Huang, B. J. Braams, J. M. Bowman, R. E. Kelly, J. Tennyson, G. C. Groenenboom, A. van der Avoird, *The Journal of chemical physics* 2008, 128, 034312.
- [22] A. Shank, Y. Wang, A. Kaledin, B. J. Braams, J. M. Bowman, The Journal of chemical physics 2009, 130, 144314.
- [23] R. E. Kelly, J. Tennyson, G. C. Groenenboom, A. van der Avoird, Journal of Quantitative Spectroscopy and Radiative Transfer 2010, 111, 1262-1276.
- [24] C. Leforestier, K. Szalewicz, A. Van Der Avoird, The Journal of chemical physics 2012, 137, 014305.
- [25] C. Leforestier, The Journal of chemical physics 2014, 140, 074106.
- [26] D. Hankins, J. Moskowitz, F. Stillinger, The Journal of Chemical Physics 1970, 53, 4544-4554.
- [27] J. Cui, H. Liu, K. D. Jordan, The Journal of Physical Chemistry B 2006, 110. 18872-18878.
- [28] U. Góra, R. Podeszwa, W. Cencek, K. Szalewicz, The Journal of chemical physics 2011, 135, 224102.
- [29] D. M. Bates, J. R. Smith, G. S. Tschumper, *Journal of chemical theory and computation* 2011, 7, 2753-2760.
- [30] X. Huang, B. J. Braams, J. M. Bowman, The Journal of Physical Chemistry A 2006, 110, 445-451.
- [31] R. Schwan, C. Qu, D. Mani, N. Pal, L. van der Meer, B. Redlich, C. Leforestier, J. M. Bowman, G. Schwaab, M. Havenith, Angewandte Chemie International Edition 2019, 58, 13119-13126.
- [32] Y. Wang, B. C. Shepler, B. J. Braams, J. M. Bowman, The Journal of chemical physics 2009, 131, 054511.
- [33] Y. Wang, X. Huang, B. C. Shepler, B. J. Braams, J. M. Bowman, The Journal of chemical physics 2011, 134, 094509.
- [34] B. E. Rocher-Casterline, L. C. Ch'ng, A. K. Mollner, H. Reisler, Vol. 134, American Institute of Physics, 2011, p. 211101.
- [35] L. C. Ch'ng, A. K. Samanta, Y. Wang, J. M. Bowman, H. Reisler, The Journal of Physical Chemistry A 2013, 117, 7207-7216.
- [36] G. A. Cisneros, K. T. Wikfeldt, L. Ojamäe, J. Lu, Y. Xu, H. Torabifard, A. P. Bartok, G. Csanyi, V. Molinero, F. Paesani, *Chemical reviews* 2016, 116, 7501-7528.
- [37] A. J. Tursi, E. R. Nixon, The Journal of Chemical Physics 1970, 52, 1521-1528.
- [38] T. R. Dyke, J. Muenter, The Journal of Chemical Physics 1972, 57, 5011-5012.
- [39] L. Fredin, B. Nelander, G. Ribbegård, The Journal of Chemical Physics 1977, 66, 4065-4072.
- [40] M. Vernon, D. Krajnovich, H. Kwok, J. Lisy, Y. Shen, Y.-T. Lee, The Journal of Chemical Physics 1982, 77, 47-57.
- [41] R. H. Page, 1984
- [42] D. Coker, R. Miller, R. Watts, The Journal of chemical physics 1985, 82, 3554-3562.

- [43] Z. Huang, R. Miller, The Journal of chemical physics 1989, 91, 6613-6631
- [44] J. Paul, R. Provencal, C. Chapo, K. Roth, R. Casaes, R. Saykally, The Journal of Physical Chemistry A 1999, 103, 2972-2974.
- [45] M. Schütz, T. Bürgi, S. Leutwyler, H. B. Bürgi, The Journal of chemical physics 1993, 99, 5228-5238.
- [46] D. J. Wales, Journal of the American Chemical Society 1993, 115, 11180-11190.
- [47] T. R. Walsh, D. J. Wales, Journal of the Chemical Society, Faraday Transactions 1996, 92, 2505-2517.
- [48] A. van der Avoird, E. Olthof, P. Wormer, The Journal of chemical physics 1996, 105, 8034-8050.
- [49] T. Taketsugu, D. J. Wales, Molecular Physics 2002, 100, 2793-2806.
- [50] H. C. Longuet-Higgins, Molecular Physics 1963, 6, 445-460.
- [51] M. G. Brown, M. R. Viant, R. P. McLaughlin, C. J. Keoshian, E. Michael, J. D. Cruzan, R. J. Saykally, A. van der Avoird, *The Journal of chemical physics* 1999, 111, 7789-7800.
- [52] F. N. Keutsch, L. B. Braly, M. G. Brown, H. A. Harker, P. B. Petersen, C. Leforestier, R. J. Saykally, *The Journal of chemical physics* 2003, 119, 8927-8937.
- [53] J. A. Anderson, K. Crager, L. Fedoroff, G. S. Tschumper, The Journal of chemical physics 2004, 121, 11023-11029.
- [54] K. Liu, M. J. Elrod, J. G. Loeser, J. Cruzan, N. Pugliano, M. Brown, J. Rzepiela, R. J. Saykally, Faraday Discussions 1994, 97, 35-41.
- [55] S. Suzuki, G. A. Blake, Chemical physics letters **1994**, 229, 499-505.
- [56] M. R. Viant, J. D. Cruzan, D. D. Lucas, M. G. Brown, K. Liu, R. J. Saykally, The Journal of Physical Chemistry A 1997, 101, 9032-9041.
- [57] M. R. Viant, M. G. Brown, J. D. Cruzan, R. J. Saykally, M. Geleijns, A. van der Avoird, The Journal of chemical physics 1999, 110, 4369-4381.
- [58] F. N. Keutsch, E. N. Karyakin, R. J. Saykally, A. van der Avoird, The Journal of Chemical Physics 2001, 114, 3988-3993.
- [59] J.-x. Han, L. K. Takahashi, W. Lin, E. Lee, F. N. Keutsch, R. J. Saykally, Chemical physics letters 2006, 423, 344-351.
- [60] D. Sabo, Z. Bačić, T. Bürgi, S. Leutwyler, Chemical physics letters 1995, 244, 283-294.
- [61] F. N. Keutsch, M. G. Brown, P. B. Petersen, R. J. Saykally, M. Geleijns, A. Van Der Avoird, *The Journal of Chemical Physics* 2001, 114, 3994-4004
- [62] J. P. Toennies, A. F. Vilesov, Annual review of physical chemistry 1998, 49, 1-41.
- [63] C. Callegari, K. K. Lehmann, R. Schmied, G. Scoles, The Journal of Chemical Physics 2001, 115, 10090-10110.
- [64] J. P. Toennies, A. F. Vilesov, Angewandte Chemie International Edition 2004, 43, 2622-2648.
- [65] F. Stienkemeier, K. K. Lehmann, Journal of Physics B: Atomic, Molecular and Optical Physics 2006, 39, R127.
- [66] M. Choi, G. Douberly, T. Falconer, W. Lewis, C. Lindsay, J. Merritt, P. Stiles, R. Miller, *International Reviews in Physical Chemistry* 2006, 25, 15-75.
- [67] M. Hartmann, R. Miller, J. Toennies, A. Vilesov, *Physical review letters* 1995, 75, 1566.
- [68] C. J. Burnham, S. S. Xantheas, M. A. Miller, B. E. Applegate, R. E. Miller, The Journal of chemical physics 2002, 117, 1109-1122.
- [69] C. Lindsay, G. Douberly, R. Miller, Journal of molecular structure 2006, 786, 96-104.
- [70] K. E. Kuyanov, M. N. Slipchenko, A. F. Vilesov, Chemical physics letters 2006, 427, 5-9.
- [71] K. Kuyanov-Prozument, M. Y. Choi, A. F. Vilesov, The Journal of chemical physics 2010, 132, 014304.
- [72] R. Schwan, M. Kaufmann, D. Leicht, G. Schwaab, M. Havenith, Physical Chemistry Chemical Physics 2016, 18, 24063-24069.
- [73] D. Mani, T. Fischer, R. Schwan, A. Dey, B. Redlich, A. Van Der Meer, G. Schwaab, M. Havenith, Rsc Advances 2017, 7, 54318-54325.
- [74] W. Klopper, M. Schütz, H. P. Lüthi, S. Leutwyler, The Journal of chemical physics 1995, 103, 1085-1098.
- [75] F. N. Keutsch, R. J. Saykally, D. J. Wales, The Journal of chemical physics 2002, 117, 8823-8835.
- [76] J. O. Richardson, S. C. Althorpe, D. J. Wales, The Journal of chemical physics 2011, 135, 124109.
- [77] C. L. Vaillant, D. J. Wales, S. C. Althorpe, The journal of physical chemistry letters 2019, 10, 7300-7304.

- [78] M. Eraković, C. L. Vaillant, M. T. Cvitaš, The Journal of Chemical Physics 2020, 152, 084111.
- [79] A. van der Avoird, K. Szalewicz, The Journal of chemical physics 2008, 128, 014302.